

## Research Paper

# Long non-coding RNA DANCR stabilizes HIF-1 $\alpha$ and promotes metastasis by interacting with NF90/NF45 complex in nasopharyngeal carcinoma

Xin Wen\*, Xu Liu\*, Yan-Ping Mao\*, Xiao-Jing Yang\*, Ya-Qin Wang, Pan-Pan Zhang, Yuan Lei, Xiao-Hong Hong, Qing-Mei He, Jun Ma<sup>✉</sup>, Na Liu<sup>✉</sup>, Ying-Qin Li<sup>✉</sup>

Sun Yat-sen University Cancer Center; State Key Laboratory of Oncology in South China; Collaborative Innovation Center of Cancer Medicine; Guangdong Key Laboratory of Nasopharyngeal Carcinoma Diagnosis and Therapy, No. 651 Dongfeng Road East, Guangzhou 510060, People's Republic of China

\*These authors contributed equally to this article.

✉ Corresponding authors: Ying-Qin Li (e-mail: liyingq@sysucc.org.cn), Na Liu (e-mail: liun1@sysucc.org.cn) and Jun Ma (e-mail: majun2@mail.sysu.edu.cn). Sun Yat-sen University Cancer Center; State Key Laboratory of Oncology in South China; Collaborative Innovation Center of Cancer Medicine; Guangdong Key Laboratory of Nasopharyngeal Carcinoma Diagnosis and Therapy, 651 Dongfeng Road East, Guangzhou 510060, People's Republic of China. Fax: +86-20-87343295; Telephone: +86-20-87343469.

© Ivyspring International Publisher. This is an open access article distributed under the terms of the Creative Commons Attribution (CC BY-NC) license (<https://creativecommons.org/licenses/by-nc/4.0/>). See <http://ivyspring.com/terms> for full terms and conditions.

Received: 2018.07.15; Accepted: 2018.10.17; Published: 2018.11.10

## Abstract

Long noncoding RNAs (lncRNAs) play an important role in the development and progression of cancers. However, the clinical significances of lncRNAs and their functions and mechanisms in nasopharyngeal carcinoma (NPC) remain largely unclear.

**Methods:** Quantitative RT-PCR was used to determine DANCR expression and Kaplan-Meier curves were used to evaluate its prognostic value. RNA sequencing followed by bioinformatic analysis was performed to determine the potential function of DANCR. *In vitro* and *in vivo* experiments were conducted to investigate its biological effects. DANCR-interacting proteins were identified by RNA pull-down assay followed by mass spectrometry and western blotting, and then confirmed by RNA immunoprecipitation (RIP) assays.

**Results:** Our previous microarray analysis identified a metastasis-associated lncRNA DANCR. Here, we found that DANCR was upregulated in NPC, especially in those with lymph node metastasis, and its upregulation could predict poor survival. We then constructed a prognostic predictive model. RNA sequencing followed by bioinformatic analysis revealed that DANCR was responsible for NPC metastasis and hypoxia phenotype. Functional studies showed that DANCR promoted NPC cell invasion and metastasis *in vitro* and *in vivo*. Further investigation suggested that DANCR could increase HIF-1 $\alpha$  mRNA stability through interacting with the NF90/NF45 complex. Additionally, overexpression of HIF-1 $\alpha$  in DANCR knockdown cells restored its suppressive effects on NPC cell migration and invasion.

**Conclusions:** Taken together, our results suggest that DANCR acts as a prognostic biomarker and increases HIF-1 $\alpha$  mRNA stability by interacting with NF90/NF45, leading to metastasis and disease progression of NPC.

Key words: nasopharyngeal carcinoma, metastasis, DANCR, NF90, HIF-1 $\alpha$

## Introduction

Nasopharyngeal carcinoma (NPC), which originates from the nasopharynx epitheliums, is one of the most prevalent malignancies in Southeast Asia

and Southern China [1, 2]. With the advent of intensity-modulated radiotherapy and combined chemoradiotherapy, local and regional controls have

been substantially improved, and distant metastasis becomes the major cause of treatment failure and cancer-related death in NPC [3, 4]. Moreover, the outcomes of salvage treatment for NPC patients that have developed distant metastasis remain frustrating [5], with a median survival about 12 months [6]. Therefore, a predictive biomarker and an understanding of its specific mechanisms in NPC metastasis are urgently required for the development of individualized therapy for NPC patients.

To date, tumor-node-metastasis (TNM) staging system is regarded as the key principle for clinical therapeutic decisions based on risk stratification and prognostic prediction. However, this anatomic-based staging system cannot reflect an individual's tumor heterogeneity and thus it is imperfect and inaccurate for predicting NPC patients who will develop distant metastasis [7, 8]. It is worth noting that growing evidence suggests that molecular biomarkers can serve as prognostic indicators and guide treatment decision for cancer patients. A great amount of effort has been made to seek for biomarkers for predicting metastasis of NPC, such as EBV-DNA, LDH, miRNA or gene expression signatures [3, 9-11]. However, there is still a need to identify novel biomarkers to guide individualized therapy for NPC patients.

Long non-coding RNAs (lncRNAs) are a group of RNA molecules that are longer than 200 nucleotides and lack protein-coding capacity. They can act as signals, guides, scaffolds or decoys of other biological molecules [12] and regulate various biological processes, such as cell proliferation, apoptosis, invasion and stem cell pluripotency [13-16]. Growing evidence indicates that lncRNAs exhibit aberrant expression in numerous cancers and are correlated with tumor progression and metastasis [17, 18]. In a recent study, based on genome-wide lncRNA expression analysis, we found that lncRNA DANCR (differentiation antagonizing non-protein coding RNA) was upregulated in high metastatic NPC cell lines [19]. DANCR was firstly identified as a suppressor in the progression of epidermal cell differentiation [20], and it functions as an oncogenic driver in several types of cancers [21, 22]. However, the biological functions and clinical significance of DANCR in NPC have not been established yet.

In this study, we found that DANCR was upregulated in NPC, especially in those with lymph node metastasis, and it could predict poor survival. We then constructed a prognostic model based on DANCR expression and N stage. RNA-sequencing followed by bioinformatic analysis revealed that DANCR was responsible for metastasis and hypoxia phenotype. Furthermore, DANCR promoted NPC cell invasion and metastasis through interacting with

NF90/NF45 complex to increase HIF-1 $\alpha$  mRNA stability. Thus, we establish a novel DANCR regulation mechanism promoting NPC development and provide a prognostic factor as well as a promising therapeutic target for NPC.

## Methods

### Clinical specimens

This study was approved by the Institutional Ethical Review Boards of the Sun Yat-sen University Cancer Center (GZR2017-059) and written informed consents were obtained from all patients. Nine freshly frozen normal nasopharyngeal epithelial tissues and 14 NPC biopsy tissues were collected from Sun Yat-sen University Cancer Center (Guangzhou, China). In addition, a total of 212 formalin-fixed paraffin-embedded (FFPE) NPC specimens were also obtained from the Sun Yat-sen University Cancer Center between January 2006 and December 2009. All of the patients were diagnosed as non-metastatic NPC and none of them received any anti-tumor therapy before biopsy. All of the patients were restaged according to the 8<sup>th</sup> edition of the American Joint Committee on Cancer (AJCC) staging manual. Detailed information about clinicopathological characteristics of all patients were collected and the median follow-up time was 73.4 months (range, 2.6 to 114.9 months).

### Cell culture

Human NPC cell lines (SUNE-1, HONE-1, CNE-1, CNE-2, HNE-1, 5-8F, 6-10B and C666-1) were provided by Professor Musheng Zeng (Sun Yat-sen University Cancer Center, Guangzhou, China) and maintained in RPMI-1640 (Gibco, Life Technologies, Carlsbad, CA, USA) supplemented with 10% fetal bovine serum (FBS; Gibco). The other two human NPC cell lines (S18 and S26) were obtained from Professor Chaonan Qian (Sun Yat-sen University Cancer Center), and cultured in DMEM (Invitrogen, Grand Island, NY, USA) supplemented with 10% FBS. The human immortalized nasopharyngeal epithelial cell line (NP69) was grown in keratinocyte/serum-free medium (Invitrogen) supplemented with bovine pituitary extract (BD Biosciences, San Diego, CA, USA). 293FT cells were maintained in DMEM supplemented with 10% FBS.

### RNA extraction, reverse transcription and quantitative PCR

TRIzol reagent (Invitrogen) was used to extract total RNA from NPC cell lines and freshly-frozen NPC samples. QIAGEN FFPE RNeasy kit (QIAGEN GmbH, Hilden, Germany) was used to extract total RNA from FFPE NPC samples. The RNA amount and

quality were measured using a NanoDropND-2000 spectrophotometer (Thermo Scientific, Rockford, IL, USA). Reverse transcription was performed using reverse transcriptase (Promega, Madison, WI, USA) and random primers (Promega) for lncRNAs and mRNAs. Then, quantitative PCR reactions were conducted with SYBR Green qPCR SuperMix-UDG reagents (Invitrogen) on the CFX96 Touch sequence detection system (Bio-Rad, Hercules, CA, USA). GAPDH and  $\beta$ -actin were used as the normalization controls for NPC cell lines and freshly frozen specimens or FFPE samples, respectively. The relative expression levels were calculated using  $2^{-\Delta\Delta CT}$  method [23]. Specific primers for lncRNAs and mRNAs are shown in Table S1.

### Oligonucleotide and plasmid transfection and stable cell line generations

Effective siRNA oligonucleotides that targeted DANCR, NF45 or NF90 were purchased from RiboBio (Guangzhou, China). LV3 lentiviral vectors that encode short hairpin RNA (shRNA) targeting DANCR or non-specific control were constructed by GenePharma (Suzhou, China). The siRNA and shRNA sequences are shown in Table S1. The pENTER-vector, pENTER-DANCR and pENTER-HIF-1 $\alpha$  plasmids were purchased from Vigene Biosciences (Jinan, China). All of the plasmids were confirmed through DNA sequencing.

The synthesized short hairpin RNA targeting DANCR (shDANCR) or control shRNA were cloned into pSuper-retro-puromycin vectors (Addgene, Cambridge, MA, USA). NPC cells were transfected with oligonucleotides (100 nM) or plasmids (2  $\mu$ g) using Lipofectamine 3000 or Lipofectamine 2000 reagents (Invitrogen). The cells were harvested for assays 48 h after transfection. SUNE-1 cell lines stably expressing shDANCR or vector were generated after lentiviral infection by 293FT cells and selected by 0.5  $\mu$ g/mL puromycin.

### RNA sequencing and bioinformatic analysis

Total RNA was isolated from SUNE-1 transfected with siDANCR-1 or scramble control and the RNA quality was evaluated using Agilent Bioanalyzer 2100 (Agilent technologies, CA, USA). Qualified RNA was then purified by RNA Clean XP Kit (Beckman Coulter, CA, USA) and RNase-Free DNase Set (QIAGEN). Next, we constructed Illumina sequencing libraries according to the modified strand-specific RNA sequencing protocol. Briefly, we isolated non-coding RNA and coding RNA from 3  $\mu$ g of purified total RNA using a ribo-zero kit for rRNA removal. After isolation, we eluted and fragmented the RNA samples at 94 °C for 8 min with

Elute-Prime-Fragment Mix. Subsequently, we synthesized the first-strand cDNA using SuperScript II (Invitrogen). Then, the product mixed with Second Strand Marking Master Mix was incubated at 16 °C for 1 h to synthesize the second-strand cDNA. After 3'ends adenylation, we ligated the DNA fragments with TruSeq adapters and the product was amplified using TruSeq PCR primers. Then, the libraries were loaded on cBot (Illumina, San Diego, CA, USA) to generate a cluster and subsequently sequenced on the HiSeq X ten (Illumina) platform at the Longsee medical Corporation (Guangzhou, China).

RNA-seq reads were mapped to the human reference genome sequence (hg38) assembly by Hisat2 (Version 2.1.0). Stringtie (version 1.3.3) was used to count the number of fragments of each known gene downloaded from Ensembl (Homo sapiens GRCh38). After mapping, we removed genes with fewer than 10 fragments in all of the samples and identified differentially expressed genes using R/Bioconductor package edge R (version 3.0.8). Thresholds of  $P < 0.05$  and fold change  $\geq 1.5$  were used to identify differentially expressed genes.

The differentially expressed genes were used to perform KEGG (Kyoto Encyclopedia of Genes and Genomes) pathway analysis and GO (Gene ontology) analysis using DAVID software (<https://david.ncifcrf.gov/>). Two-sided or Bonferroni-corrected Fisher's exact tests were used to calculate the  $P$ -values of KEGG pathways or GO terms, respectively. Furthermore, we performed gene set enrichment analysis (GSEA) to identify the biological function enriched in NPC with DANCR knockdown. H collection (hallmark gene sets,  $n=50$ ) and C2 collection of chemical and genetic perturbations ( $n=3409$ ) from Molecular Signatures Database-MsigDB (<http://www.broad.mit.edu/gsea/msigdb/index.jsp>) were used for enrichment analysis. A threshold of  $P < 0.05$  and  $FDR \leq 0.25$  was used to select significant items. All of the data were deposited in the Gene Expression Omnibus of National Center for Biotechnology Information (GSE117415).

### Wound healing, Transwell migration and invasion assays

For the wound healing assays, transfected NPC cells were grown to near confluence in six-well plates and then subjected to serum-free medium for 24 h. Artificial wounds were scratched on the monolayers, and images were captured at 0 h and 24 h. Cell migrative and invasive abilities were detected with Transwell chambers (8- $\mu$ m pores; Corning, Corning, NY, USA) that coated without or with Matrigel (BD Biosciences). NPC cells ( $5 \times 10^4$  or  $1 \times 10^5$ ) suspended in serum-free medium were plated in the upper

chambers. Medium supplemented with 10% FBS was placed in the lower chambers. After incubation for 16 or 24 h, the migrated or invaded cells were fixed, stained and counted through an inverted microscope.

### CCK8 and colony formation assays

For CCK-8 assay,  $1 \times 10^3$  cells in 100  $\mu$ L medium were cultured per well in 96-well plates. Then, 10  $\mu$ L CCK-8 solution (DOJINDO, Japan) was added into each well. After the plates were incubated for 2 h, we used a spectrophotometric plate reader (BioTek ELX800, USA) to measure the absorbance at 450 nm for each sample. For colony formation assay, 400 cells in 2 mL medium were seeded in 6-well plates and cultured for 7 or 12 days. Cell colonies were then washed, fixed, stained and counted.

### RNA pull-down assay and mass spectrometry analysis

Full-length sense and antisense of DANCR RNA or its fragments (1-300, 301-904, 1-600 and 601-904) were *in vitro* transcribed with MEGAscript™ T7 Transcription Kit (Thermo Fisher Scientific, Waltham, MA, USA). The transcripts were then labeled with biotin using Pierce™ RNA 3' End Desthiobiotinylation Kit (Thermo Fisher Scientific). After obtaining the whole lysates from SUNE-1 cells, we performed a pull-down assay using Pierce™ Magnetic RNA-Protein Pull-Down Kit (Thermo Fisher Scientific) according to the manufacturer's protocol. Mass spectrometry was performed by Huijun Biotechnology (China).

### Western blotting assay

We harvested cells and extracted proteins from NPC cells. Samples were then separated in 10-14% SDS-PAGE gels and transferred to PVDF membranes (Merck Millipore, Billerica, MA, USA). After blocking in 5% defatted milk, the membranes were incubated with primary antibodies overnight at 4 °C. Following incubation with secondary antibodies, signals were detected using the ECL detection system (Thermo Fisher Scientific). The antibodies used in western blotting assays can be found in **Table S2**.

### RNA immunoprecipitation

Magna RIP™ RNA-Binding Protein Immunoprecipitation Kit (Merck Millipore) was used for RNA immunoprecipitation (RIP) assays according to the manufacturer's instructions. NF45 and NF90 antibodies used for RIP are displayed in **Table S2**. The co-precipitated RNAs were quantified through standard quantitative RT-PCR. The primers used for detecting DANCR and HIF-1 $\alpha$  are shown in **Table S1**.

### In vivo xenograft tumor models

All of the animal experiments were performed according to guidelines approved by the Institutional Animal Care and Use Ethics Committee of the Sun Yat-sen University Cancer Center (L102012017004W). Six-week-old female BALB/c nude mice were obtained from the Medical Experimental Animal Center of Guangdong Province (Guangzhou, China). To establish an inguinal lymph node metastasis model, 30  $\mu$ L PBS containing  $2 \times 10^5$  SUNE1 cells stably expressing shDANCR or control shRNA was transplanted into the foot pads of nude mice (n=6 per group). After 6 weeks, mice were sacrificed and their inguinal lymph nodes and primary tumors were dissected. For the *in vivo* lung metastasis colonization model, 200  $\mu$ L PBS containing  $1 \times 10^6$  SUNE1 cells stably expressing shDANCR or control shRNA was injected into the mice by the tail vein (n=5 per group). After 8 weeks, the mice were sacrificed and their lung tissues were detached. All of the dissected tissue samples were paraffin-embedded, sectioned and stained with H&E. Additionally, immunohistochemistry (IHC) staining was performed on the inguinal lymph nodes using an anti-pan-cytokeratin antibody (Thermo Fisher Scientific, Waltham, MA, USA).

### Statistical analysis

All of the data are presented as the mean  $\pm$  SD from at least 3 independent experiments. Student's *t*-test was used to compare continuous variables and  $\chi^2$  or Fisher's exact tests were used to compare categorical variables. Receiver operating characteristic (ROC) curve analysis was performed to determine the optimal cutoff value for the classification of high or low DANCR expression. The Kaplan-Meier method was used to estimate overall, disease-free and distant metastasis-free survivals, and the *P*-values were calculated using the log-rank test. Cox proportional hazards regression model was used to determine the independent prognostic factors. *P* < 0.05 were considered significant. The above statistical analyses were conducted with SPSS software version 22.0 (IBM, Chicago, IL, USA).

## Results

**LncRNA DANCR is upregulated in NPC and is associated with poor prognosis**

Based on our previous genome-wide analysis of lncRNA expression (GSE89804) [19], we found that lncRNA DANCR was upregulated in NPC cell lines with high metastatic potential (5-8F and S18) compared with those with low metastatic potential (6-10B and S26, **Figure S1A**), which was confirmed by

quantitative RT-PCR (Figure S1B). We then quantified the expression level of DANCR in an immortalized nasopharyngeal epithelial cell line NP69 and 10 NPC cell lines. Significantly, high expression of DANCR was found in the NPC cell lines compared with NP69 (Figure 1A,  $P < 0.05$ ). Furthermore, we examined the expression level of DANCR in 9 freshly-frozen normal nasopharyngeal epithelial tissues and 14 NPC tissue samples. DANCR was found to be remarkably overexpressed in NPC tissues, especially in those with lymph node metastasis (Figure 1B-C,  $P < 0.05$ ). These findings indicate that DANCR might function as an oncogenic lncRNA that is involved in NPC metastasis.

To test whether the expression status of DANCR has clinical value in NPC, we performed quantitative

RT-PCR in 212 paraffin-embedded NPC biopsy tissue samples. Based on the ROC analysis, 74 (34.9%) patients had low DANCR expression and 138 (65.1%) had high DANCR expression. As shown in Table S3, high DANCR expression was significantly associated with distant metastasis ( $P = 0.011$ ) and death ( $P = 0.023$ ). However, there were no obvious associations between DANCR expression and other clinical features (all  $P > 0.05$ ). Furthermore, patients with high DANCR expression had poorer overall survival, disease-free survival and distant metastasis-free survival than those with low DANCR expression (all  $P < 0.05$ ; Figure 1D-F). Multivariate Cox regression analysis found that DANCR expression and N stage were independent prognostic factors for NPC patients (Table S4).

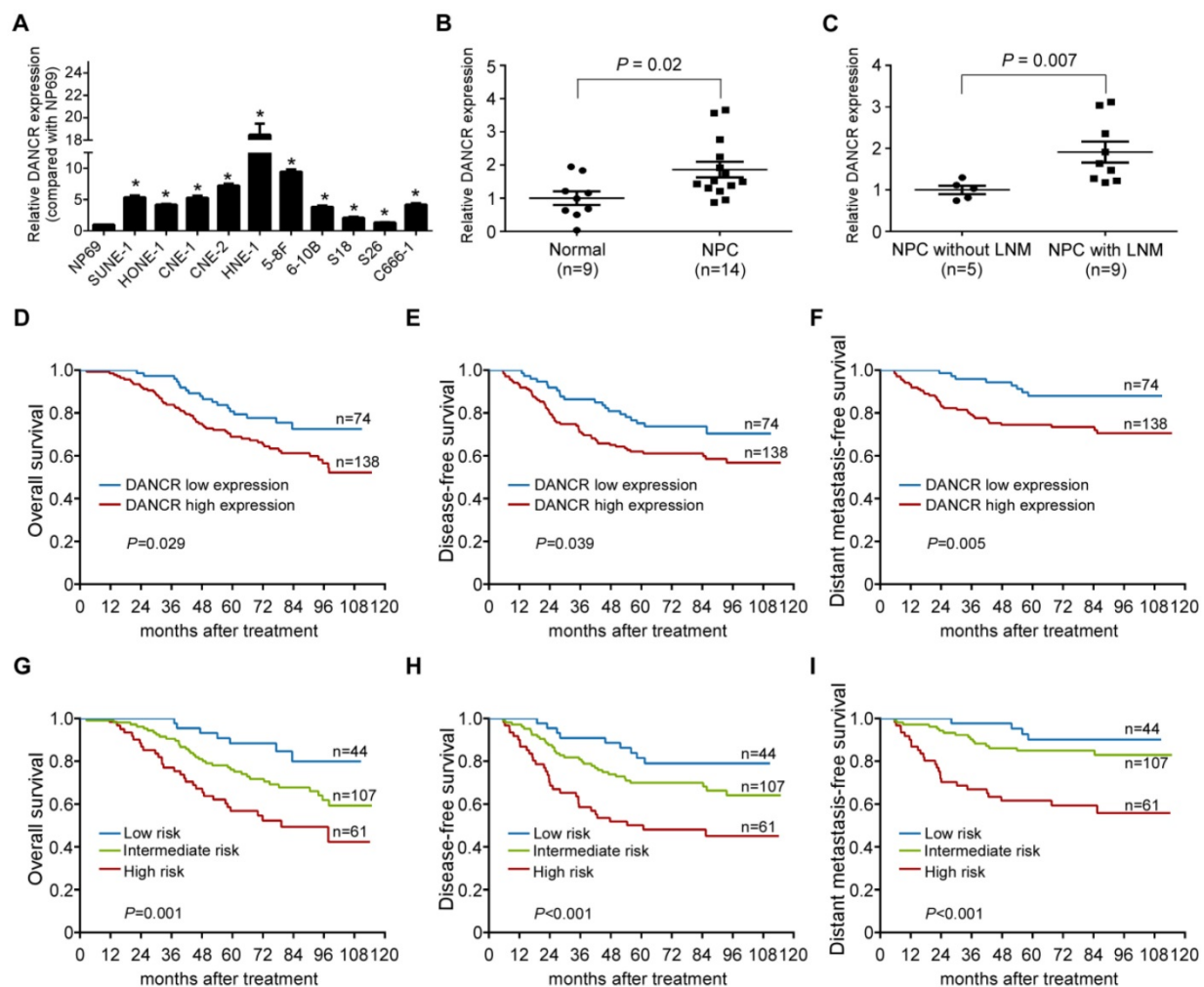


**Figure 1. lncRNA DANCR is upregulated in NPC and is associated with poor prognosis. (A)** Relative expression of DANCR measured by qRT-PCR in NP69 and 10 NPC cell lines. The experiments were independently repeated 3 times. Data are presented as mean  $\pm$  SD; Student's *t*-tests; \* $P < 0.05$ . **(B)** Relative expression of DANCR in normal nasopharyngeal epithelial (n=9) and NPC tissues (n=14). **(C)** Relative expression of DANCR in NPC tissues with (n=9) or without (n=5) lymph node metastasis. GAPDH was used as an internal control. Data are presented as mean  $\pm$  SD; Student's *t*-tests; \* $P < 0.05$ . **(D-F)** Relative DANCR expression via qRT-PCR in a cohort of 212 NPC tissues. Kaplan-Meier analysis of overall (D), disease-free (E) and distant metastasis-free survival (F) in NPC patients with low DANCR expression (n=74) and high DANCR expression (n=138). **(G-I)** Kaplan-Meier analysis of overall (G), disease-free (H) and distant metastasis-free survival (I) according to the prognostic prediction model in patients with low risk (low DANCR expression and early N stage, n=44), intermediate-risk (high DANCR expression or advanced N stage, n=107) and high-risk (high DANCR expression and advanced N stage, n=61).  $\beta$ -actin was used as the internal control. Log-rank test; \* $P < 0.05$ .

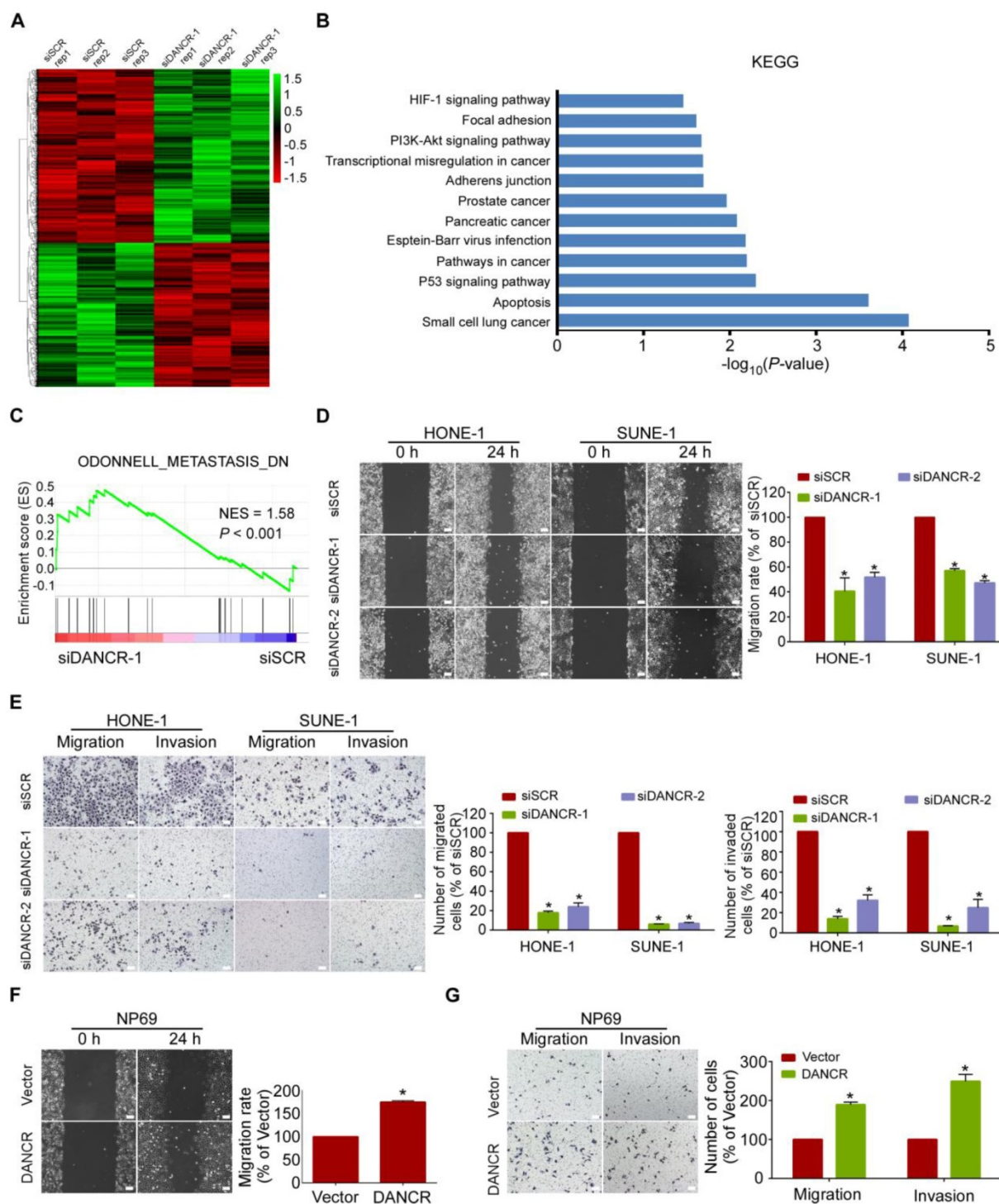


**Figure 2.** LncRNA DANCR promotes NPC cell migration and invasion *in vitro*. **(A)** Heatmap showing the genes altered ( $\geq 1.5$ -fold change) in SUNE-1 cells transfected with DANCR siRNA or scramble control, with 3 replicates. Gene expression is shown as RPKM after normalization. **(B)** KEGG pathway analysis for all dysregulated genes in SUNE-1 cells transfected with DANCR siRNA or scramble control. Cancer and metastasis-related terms were among the significant pathways for the genes dysregulated in the DANCR-silenced NPC cells. **(C)** Metastasis-related biological function enriched using gene set enrichment analysis (GSEA) in SUNE-1 cells transfected with DANCR siRNA or scramble control.  $P < 0.05$ ,  $FDR \leq 0.25$ . NES: normalized enrichment score. **(D-E)** Representative and quantification results of the wound healing (D) and Transwell migration and invasion assays (E) in HONE-1 and SUNE-1 cells transfected with DANCR siRNA or scramble control. **(F-G)** Representative and quantification results of the wound healing (F) and Transwell migration and invasion assays (G) in NP69 cells transfected with DANCR-overexpressing plasmid or vector. Scale bar, 100  $\mu\text{m}$ . Data are presented as mean  $\pm$  SD; Student's *t*-tests; \* $P < 0.05$ . The experiments were independently repeated 3 times.

We then constructed a prognostic prediction model based on DANCR expression status and N stage. Patients were stratified into 3 groups: 44

(20.7%) patients in the low-risk group (low DANCR expression and early N stage), 107 (50.5%) patients in the intermediate-risk group (high DANCR expression

or advanced N stage) and 61 (28.8%) patients in the high-risk group (high DANCR expression and advanced N stage). K-M Survival analysis showed that patients in these 3 groups exhibited significantly different survival prospects (all  $P < 0.05$ ; **Figure 1G-I**). Collectively, our findings indicate that the combination of DANCR expression with N stage is a promising signature to predict prognosis of NPC.

### LncRNA DANCR downregulation is correlated with NPC metastasis

To determine whether DANCR plays a role in NPC tumorigenesis, we firstly transfected SUNE1 cells with DANCR-specific siRNA (siDANCR-1) or a scramble control (siSCR), and then compared their gene expression differences using RNA sequencing. The results showed that 1875 genes were upregulated and 1515 genes were downregulated ( $\geq 1.5$ -fold) in SUNE-1 cells with DANCR knockdown (**Figure 2A**). KEGG and GO analyses were utilized to investigate the involved pathways activated by DANCR. The results revealed that the above differentially expressed genes were enriched in cancer- and metastasis-related terms (**Figure 2B** and **Figure S2A-C**). Moreover, GSEA found that the gene set related to Odonnell\_Metastasis\_DN (downregulated genes for lymph node metastasis in head and neck squamous cell carcinoma) was positively correlated with DANCR downregulation (**Figure 2C**). These data suggest that DANCR might be a vital regulator involved in NPC metastasis.

### LncRNA DANCR promotes NPC cell migration and invasion *in vitro*

To functionally confirm the above findings, we transiently transfected HONE-1, SUNE-1, 5-8F, and HNE-1 cells with DANCR siRNAs or scramble control, or transfected NP69,6-10B, and S26 cells with the DANCR-overexpressing plasmid or a vector control (**Figure S3A-G**). Then, wound healing and Transwell assays with or without Matrigel were performed. The data showed that silencing of DANCR significantly suppressed the migrative (**Figure 2D-E** and **Figure S4A-D**,  $P < 0.05$ ) and invasive (**Figure 2E** and **Figure S4B, D**,  $P < 0.05$ ) abilities of NPC cells. In contrast, overexpression of DANCR promoted the migration (**Figure 2F-G** and **Figure S4E-H**,  $P < 0.05$ ) and invasion (**Figure 2G** and **Figure S4F, H**,  $P < 0.05$ ) of NP69, 6-10B and S26 cells. Furthermore, CCK8 and colony-formation assays revealed that knockdown of DANCR had minimal influences on cell proliferation (**Figure S5**,  $P > 0.05$ ). These data suggest that DANCR promotes NPC cell migration and invasion but has little effect on cell proliferation.

### LncRNA DANCR binds to NF90 and NF45

Recent studies have demonstrated that lncRNAs may exert their function by interactions with specific proteins [24, 25]. To explore the underlying regulatory mechanism of DANCR, we did a biotin RNA pull-down assay followed by mass spectrometry to identify DANCR-interacting proteins (**Figure 3A-B**). The results showed that NF90 was the most enriched DANCR-binding partner; meanwhile, NF45, which can form an RNA-binding complex with NF90, was also identified (**Table S5-6**). Western blotting results validated that both NF90 and NF45 were abundant in DANCR-pull-down lysates (**Figure 3C**).

Then, deletion-mapping analysis was performed to learn about which region of DANCR is required for its binding to NF90/NF45. We found that the deletion transcripts close to the 3' region of DANCR exhibited stronger binding abilities to NF90/NF45 than those near the 5' region (**Figure 3D**, lower panel). It should be noted that more AU-rich elements, which are the canonical NF90 target sequences [26, 27], were present in the transcripts close to the 3' region of DANCR than in the 5' and central regions (**Figure 3D**, upper panel), indicating that the 3' region of DANCR might be more necessary for its interaction with NF90/NF45.

Furthermore, we validated the interaction between DANCR and NF90/NF45 through RNA immunoprecipitation (RIP) with antibodies against NF90 or NF45 in SUNE-1 cells. We found that DANCR RNA was significantly enriched using the NF90 and NF45 antibodies (**Figure 3E**). RIP-PCR also revealed that knockdown of DANCR obviously abolished the interaction between DANCR and NF90/NF45 (**Figure 3F-G**,  $P < 0.05$ ). However, knockdown of DANCR had little effect on the expression of NF90 and NF45 (**Figure 3H** and **Figure S6**). Silencing NF90 or NF45 also didn't affect the expression level of DANCR (**Figure 3I**,  $P > 0.05$ ). Altogether, our findings demonstrate a direct interaction between DANCR and NF90/NF45.

### LncRNA DANCR stabilizes HIF-1 $\alpha$ through interacting with NF90

Subsequently, to explore the functional relevance of the interaction between DANCR and NF90/NF45, we performed GSEA using the RNA-sequencing data from SUNE-1 cells that had been transfected with DANCR-specific siRNA or a scramble control. Importantly, we found that the hypoxia phenotype was positively correlated with DANCR expression (**Figure 4A-B** and **Figure S7**). Actually, a substantial subset of genes involved in hypoxia pathways were dysregulated after DANCR knockdown, including HIF-1 $\alpha$ . HIF-1 $\alpha$  functions as a

core regulator of hypoxia response by activating gene transcription. Interestingly, a gene set containing genes that are transcriptionally regulated by HIF-1 $\alpha$  (SEMENZA\_HIF1\_TARGETS) was also found to be associated with DANCR expression (Figure 4C). These results suggest that HIF-1 $\alpha$  may play a causal role in the DANCR regulation network.

To confirm the above findings, we firstly did quantitative RT-PCR and western blotting assays, and found that both the mRNA and protein of HIF-1 $\alpha$  were obviously decreased in HONE1 and SUNE1 cells

after knockdown of DANCR under hypoxic environment (Figure 4D-E). Then, to explore whether DANCR regulates HIF-1 $\alpha$  mRNA level through increasing its stability, we treated NPC cells with RNA synthesis inhibitor actinomycin D and obtained RNAs at 0 h, 1 h, and 2 h. We found that HIF-1 $\alpha$  mRNA degraded more quickly in the DANCR knockdown groups than the scramble control group (Figure 4F-G), suggesting that depletion of DANCR reduced the HIF-1 $\alpha$  mRNA stability.

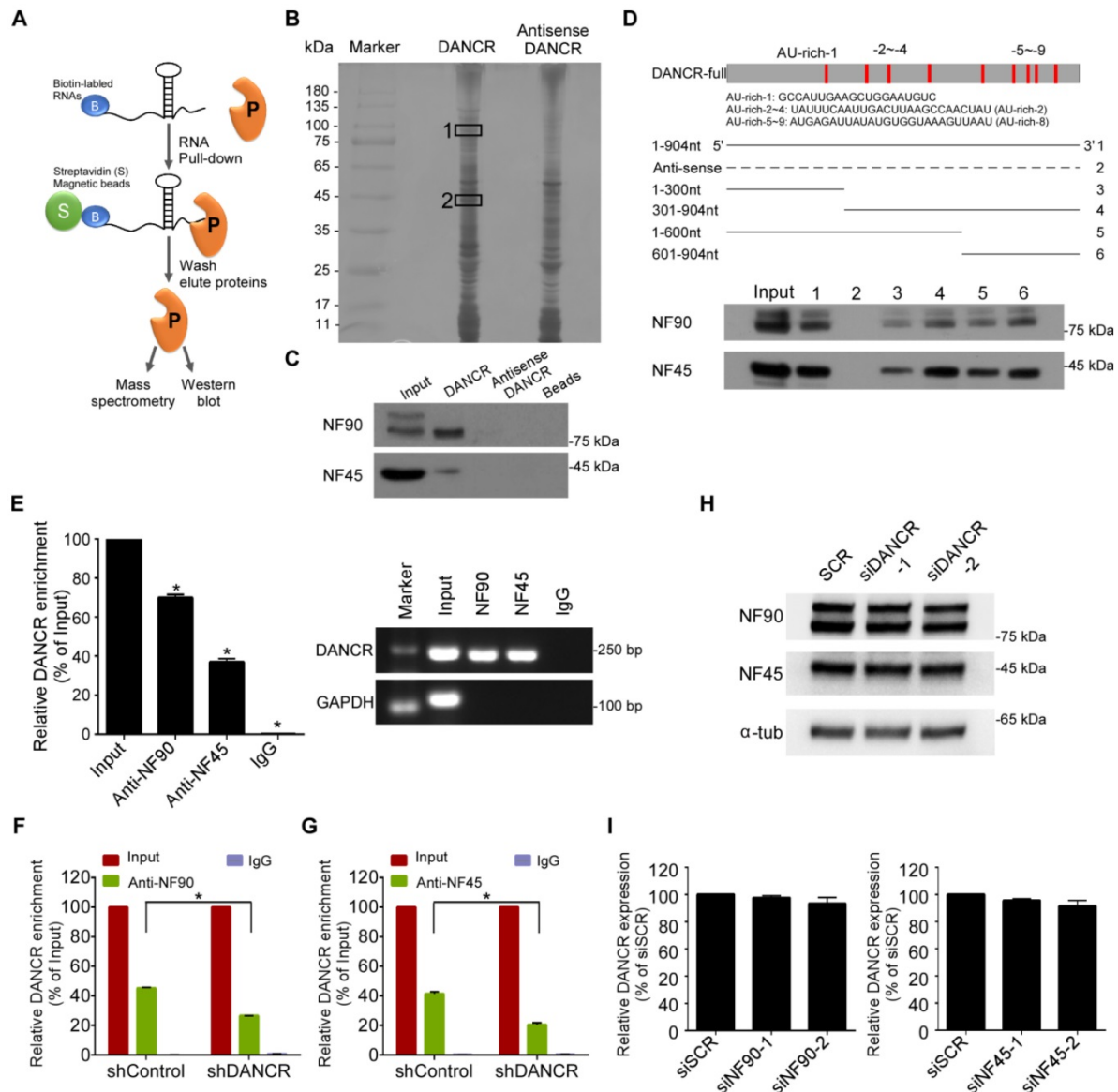


**Figure 3.** LncRNA DANCR binds to NF90 and NF45. (A) Schematic flow of the RNA pull-down assay for identification of DANCR-associated proteins. DANCR and anti-DANCR RNA were biotinylated, refolded, and incubated with SUNE-1 cell lysates. (B) Silver staining of biotinylated DANCR-associated proteins. Specific bands were excised and analyzed through mass spectrometry. NF90 and NF45 were identified as the bands unique to DANCR. (C) Western blot analysis of the specific association of NF90 and NF45 with DANCR from RNA pull-down assay. (D) Schematic of the full-length and deletion fragments of DANCR used for the precipitation of NF90 and NF45 from SUNE-1 cell lysates. AU-rich elements in DANCR transcript are shown in red (upper panel). Associated NF90 and NF45 proteins were detected by western blotting (lower panel). (E) RNA immunoprecipitation (RIP) assays were performed using NF90 or NF45 antibodies. Specific primers were used to detect DANCR or GAPDH, and RIP enrichment was determined relative to an input control. (F-G) Knockdown of DANCR decreased the interaction of DANCR with NF90 (F) and NF45 (G), as detected by RIP assay using NF90 and NF45 antibodies. (H) NF90 and NF45 expression levels were measured through western blotting after knockdown of DANCR. (I) DANCR expression level was measured by quantitative RT-PCR after knockdown of NF90 or NF45. Data are presented as mean (n=3)  $\pm$  SD; Student's t-tests; \*P<0.05.

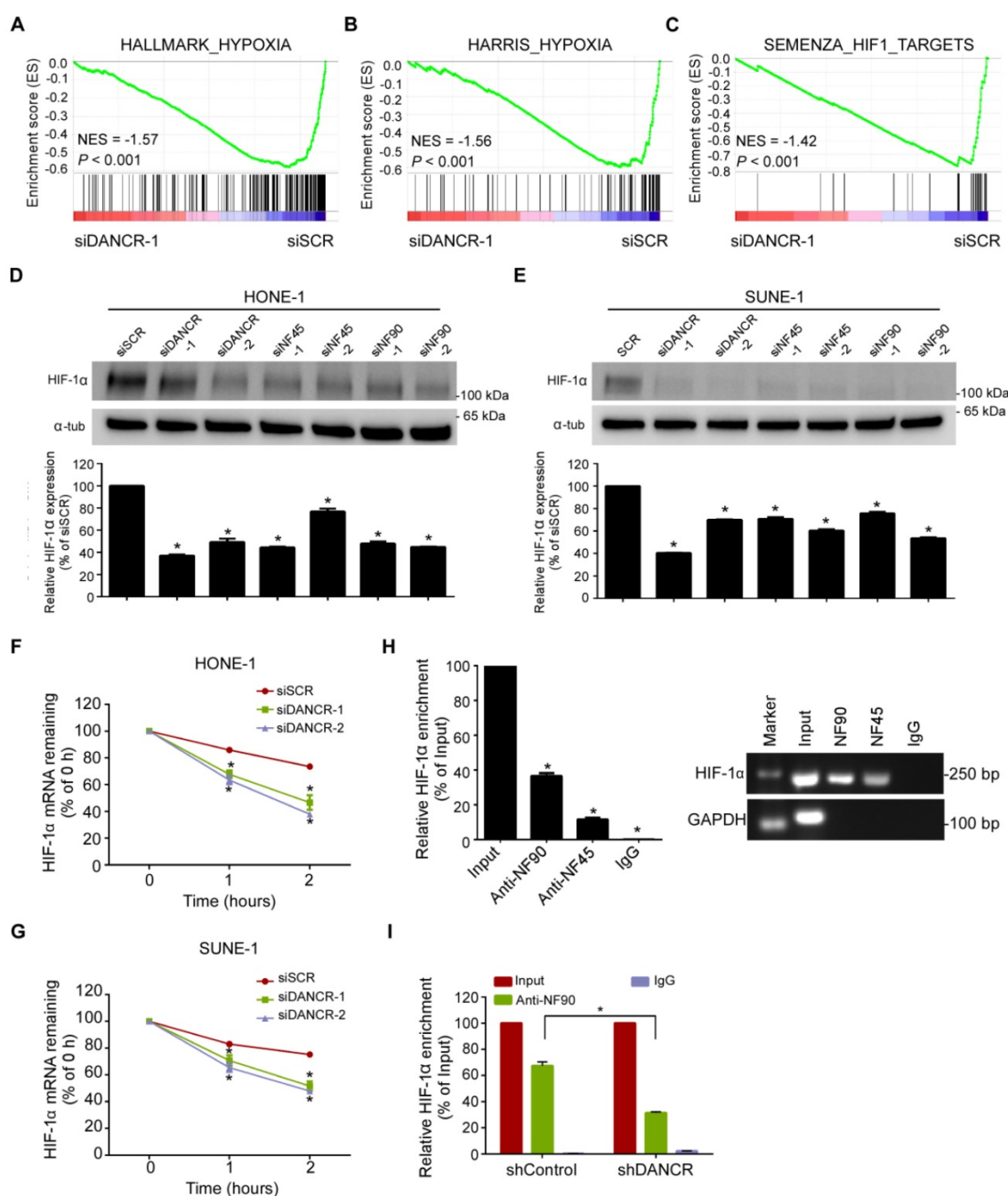


**Figure 4.** LncRNA DANCR stabilizes HIF-1α through interacting with NF90. **(A-C)** Hypoxia- and HIF-1α-related biological function enriched using gene set enrichment analysis (GSEA) in SUNE-1 cells transfected with DANCR siRNA or scramble control.  $P < 0.05$ ,  $FDR \leq 0.25$ . NES: normalized enrichment score. **(D-E)** The protein (upper panel) and mRNA (lower panel) levels of HIF-1α in HONE-1 (D) and SUNE-1 (E) cells transfected with DANCR-siRNAs, NF45-siRNAs, NF90-siRNAs or scramble control under hypoxic conditions. **(F-G)** Reduction of HIF-1α mRNA stability in DANCR knockdown HONE-1 (F) and SUNE-1 (G) cells as compared to control cells. Cells were treated with 1 μg/mL actinomycin D and RNA was isolated at 0 h, 1 h and 2 h. **(H)** RNA immunoprecipitation (RIP) assays were performed using NF90 or NF45 antibodies. Specific primers were used to detect HIF-1α or GAPDH, and RIP enrichment was determined relative to an input control. **(I)** Knockdown of DANCR decreased the interaction of HIF-1α with NF90, as detected by RIP assay using NF90 antibody. Data are presented as mean ± SD; Student's *t*-tests; \* $P < 0.05$ . The experiments were independently repeated 3 times.

NF90, as the most-enriched DANCR-binding protein, is a double-stranded RNA-binding protein and can complex with NF45 to stabilize mRNA and regulate gene expression [28]. Thus, we proposed a hypothesis that DANCR might stabilize HIF-1α mRNA stability through interacting with NF90/NF45. Indeed, western blotting and quantitative RT-PCR

revealed a remarkable reduction of HIF-1α expression in HONE-1 and SUNE-1 cells after knockdown of NF90 or NF45 under hypoxic environment (Figure 4D-E). Additionally, RIP assay confirmed the interaction between NF90/NF45 and HIF-1α (Figure 4H). Furthermore, we performed an RIP assay using NF90 antibody in SUNE-1 cells stably transfected with

DANCR shRNA or vector control and found that DANCR knockdown led to a 2.1-fold decrease in HIF-1 $\alpha$  enrichment (Figure 4I). Taken together, our results suggest that DANCR increases HIF-1 $\alpha$  mRNA stability through interacting with NF90/NF45 complex.

### LncRNA DANCR promotes NPC cell migration and invasion via HIF-1 $\alpha$

To study whether DANCR-mediated HIF-1 $\alpha$  upregulation contributes to its promotion on NPC cell migration and invasion, we did wound healing and Transwell assays with or without Matrigel under

hypoxic conditions. The results showed that hypoxia significantly increased the migrative (Figure 5A-B,  $P < 0.05$ ) and invasive (Figure 5C,  $P < 0.05$ ) abilities of NPC cells. We restored HIF-1 $\alpha$  expression in NPC cells with silenced DANCR. Strikingly, the results revealed that HIF-1 $\alpha$  co-transfection remarkably abolished the suppressive effects of DANCR depletion on hypoxia-induced NPC migration (Figure 5A-B,  $P < 0.05$ ) and invasion (Figure 5C,  $P < 0.05$ ). Our findings demonstrate that HIF-1 $\alpha$  is the functional target of DANCR in NPC.

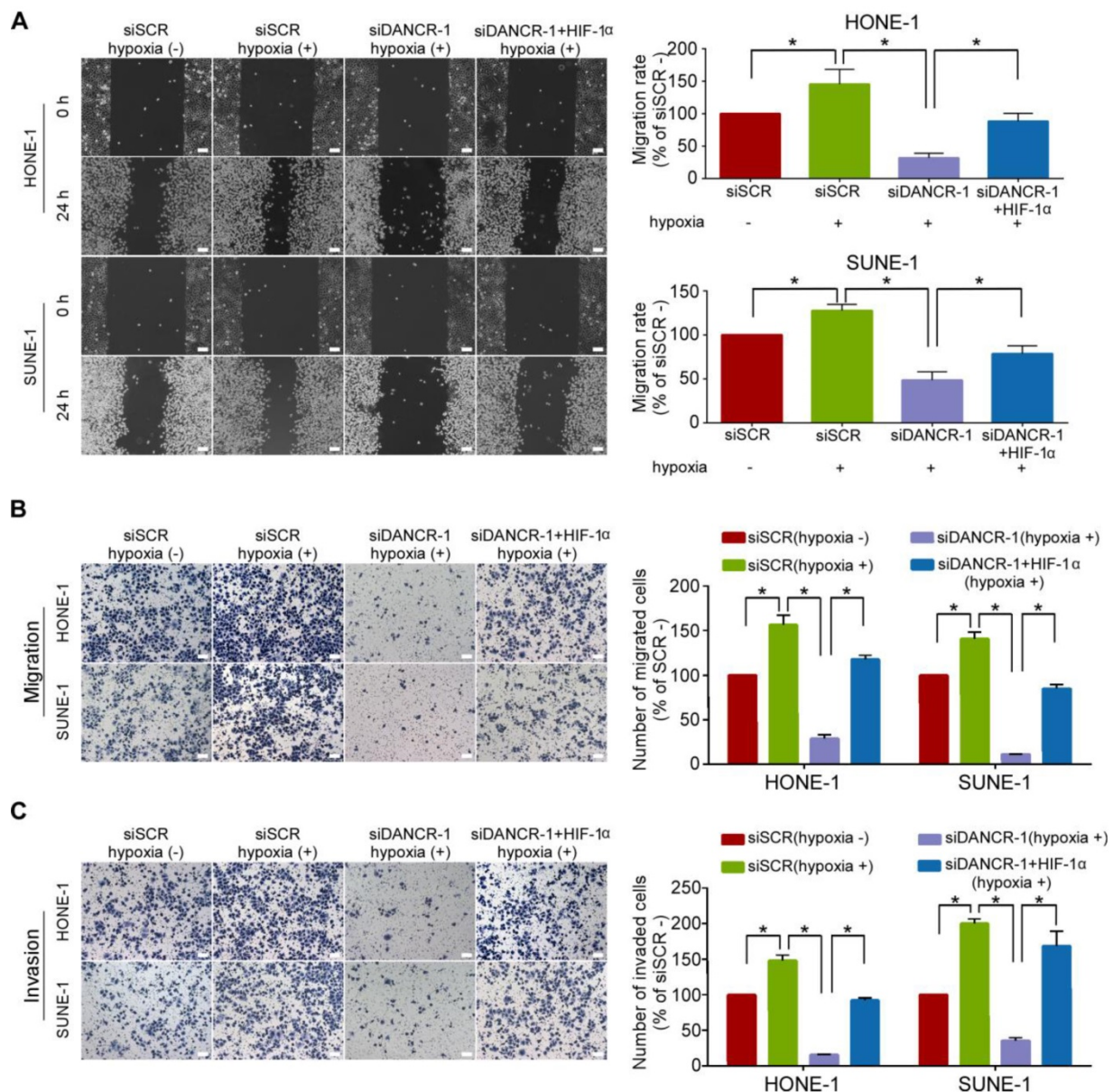


**Figure 5. LncRNA DANCR promotes NPC cell migration and invasion via HIF-1 $\alpha$ .** (A-C) Representative and quantification results of the wound healing (A), Transwell migration (B) and invasion (C) assays for HONE-1 and SUNE-1 cells under hypoxic conditions. Hypoxia induced the migration and invasion of NPC cells. The migrative and invasive abilities of NPC cells under hypoxic conditions were blocked by DANCR knockdown, and these blocked migrative and invasive abilities of NPC cells were rescued by HIF-1 $\alpha$  overexpression. Scale bar, 100  $\mu$ m. Data are presented as mean  $\pm$  SD; Student's *t*-tests; \* $P < 0.05$ . The experiments were independently repeated 3 times.

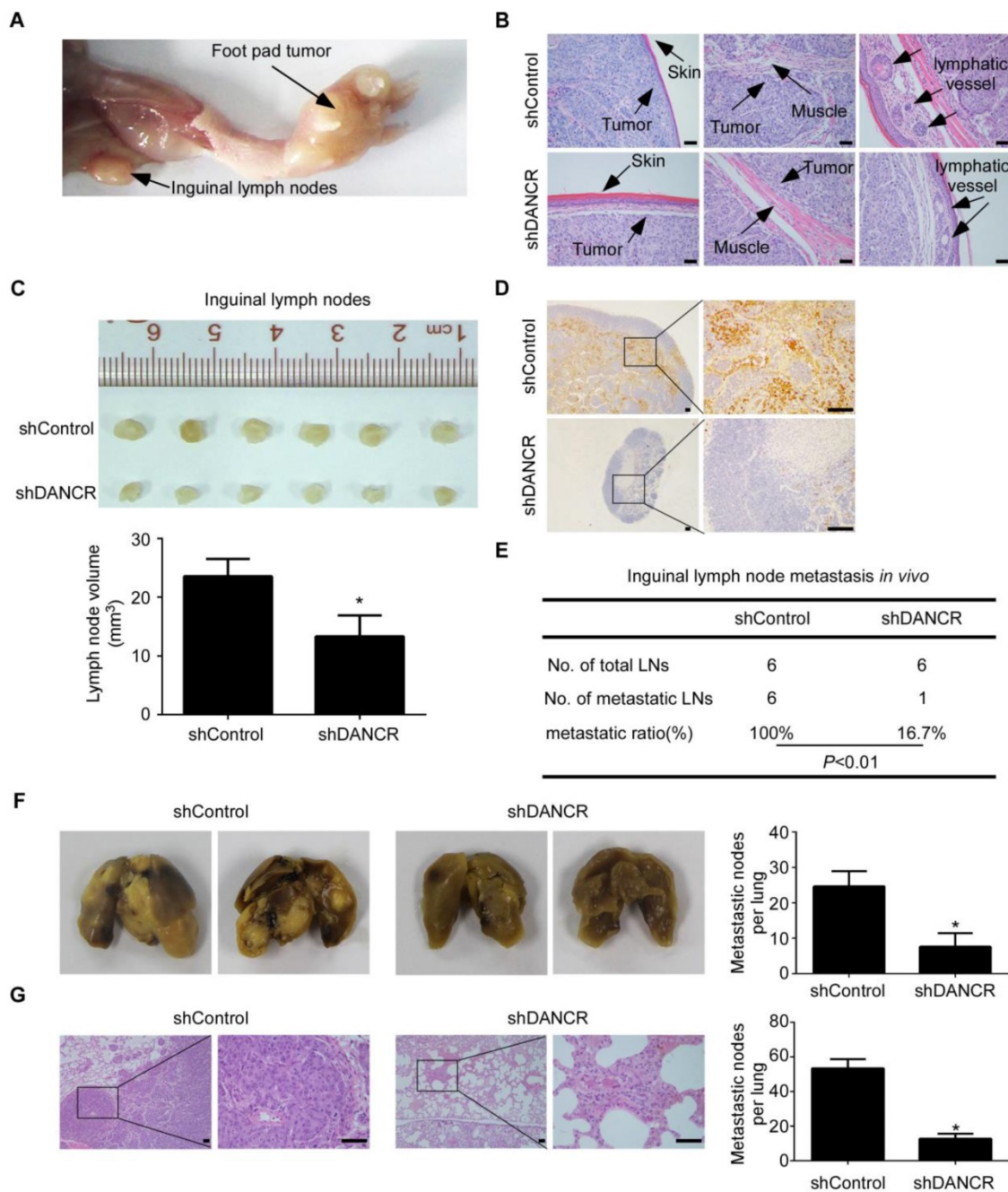


**Figure 6. LncRNA DANCR promotes NPC cell invasion and metastasis *in vivo*.** (A-E) SUNE-1 cells stably expressing shDANCR or control shRNA were transplanted into the foot pads of nude mice (n=6 per group) to construct an inguinal lymph node metastasis model. (A) Representative image of primary tumor in foot pads and metastatic inguinal lymph node. (B) Representative images of microscopic primary foot pad tumors (×200) stained with H&E. Scale bar, 50 μm. (C) Representative image (upper panel) and quantification (lower panel) of the volumes of the inguinal lymph nodes. Data are presented as mean ± SD; Student's *t*-tests; \**P*<0.05. (D) Representative images of immunohistochemistry (IHC) staining with pan-cytokeratin in inguinal lymph nodes (left panel ×40, right panel ×200). Scale bar, 100 μm. (E) Inguinal lymph node metastatic ratios. Chi-square test. (F-G) SUNE-1 cells stably expressing shDANCR or control shRNA were injected into the tail veins of nude mice (n=5 per group) to construct a lung metastasis colonization model. (F) Representative images and quantification of macroscopic metastatic nodules on the lung surfaces. Data are presented as mean ± SD; Student's *t*-tests; \**P*<0.05. (G) Representative images and quantification of microscopic metastatic nodules in the lung tissues stained with H&E (×100 and ×400). Scale bar, 50 μm. Data are presented as mean ± SD; Student's *t*-tests; \**P*<0.05.

### LncRNA DANCR promotes NPC cell invasion and metastasis *in vivo*

To evaluate the effect of DANCR on NPC metastasis *in vivo*, we constructed an inguinal lymph node metastasis model by transplanting SUNE1 cells stably expressing shDANCR or control shRNA into

the foot pads of nude mice (n=6 per group, Figure S3F). Six weeks later, the primary tumors and inguinal lymph nodes were dissected and analysed (Figure 6A). H&E staining showed that the primary tumors in the DANCR depletion group had sharp edges that expanded as spheroids and exhibited a less aggressive phenotype with invasion of the tumor cells

towards the skin, muscle and even into the lymphatic vessel (**Figure 6B**). Strikingly, the volumes of the inguinal lymph nodes in the DANCR depletion group were significantly smaller (**Figure 6C**,  $P < 0.05$ ) and had fewer pan-cytokeratin-positive tumor cells (**Figure 6D**). The metastatic inguinal lymph nodes ratio was remarkably lower in the DANCR silencing group (100.0%) than the control group (16.7%;  $P < 0.01$ ; **Figure 6E**).

We further constructed a lung metastatic colonization model by inoculating SUNE-1 cells stably expressing shDANCR or control shRNA into the tail veins of mice ( $n = 5$  per group). The nude mice were sacrificed 8 weeks later and the lung tissues were obtained. We found that the number of metastatic nodules on the lung surfaces was significantly lower in the DANCR silencing group than the control group (**Figure 6F**,  $P < 0.05$ ). In addition, H&E staining showed that the DANCR knockdown group had fewer and smaller microscopic metastatic tumor nodules (**Figure 6G**,  $P < 0.05$ ). Moreover, IHC assay showed that knockdown of DANCR had little effect on NF90 and NF45 expression (**Figure S8**). Taken together, these results suggest that DANCR promotes NPC cell invasion and metastasis *in vivo*.

## Discussion

In the present study, we evaluated the DANCR expression status and found that DANCR was upregulated in NPC, especially in those with lymph node metastasis. We also found that DANCR was associated with poor patient survival and constructed a prognostic predictive model in NPC. *In vitro* and *in vivo* functional experiments indicated that DANCR promoted NPC cell migration, invasion and metastasis, which was consistent with the function predicted by GSEA analysis. We further identified DANCR-binding proteins, NF90 and NF45, through which DANCR increased HIF-1 $\alpha$  mRNA stability, leading to NPC metastasis. Our findings elucidated the clinical value and function of DANCR in NPC, and mechanistically revealed that it may regulate gene expression at the post-transcriptional level.

Accurate prognostic prediction can efficiently guide individualized therapy for NPC, and the search for effective biomarkers warrants further studies. LncRNAs are emerging as a group of promising biomarkers for cancers because of their tissue and disease specificities [17, 29, 30]. However, the potential utilization of lncRNAs as biomarkers in NPC remains largely unknown. Here, we detected DANCR expression levels by quantitative RT-PCR in FFPE NPC tissue samples. Although the RNAs from the FFPE tissues were degraded to small pieces, they are irreplaceable for translational medicine research

because of the sufficient clinical data. Since amplification product amplicon size can influence the quantification of mRNAs and lncRNAs in FFPE samples and amplification of shorter amplicon can increase the quantification efficiency and reliability [31-33], we designed primers to generate short amplicons (~60 bp) for DANCR quantification. Survival analysis showed that NPC patients with high DANCR expression had poorer survival. Furthermore, we constructed a prognostic predictive model based on DANCR expression status and N stage. These findings suggest that DANCR is a promising prognostic biomarker, which can guide personalized therapy for NPC patients.

Recent studies report that lncRNAs are involved in the development and progression of NPC. LncRNA HOTAIR has been reported to predict poor prognosis of NPC patients [34] and promote angiogenesis by directly activating VEGFA as well as by indirect pathways [35]. Oncogenic PVT1 can induce radioresistance through regulating NPC cell apoptosis and act as a prognostic biomarker [36]. In this study, we found that DANCR was upregulated in NPC, especially in those with lymph node metastasis. Then, RNA sequencing followed by bioinformatic analysis revealed that the dysregulated genes after knockdown of DANCR were enriched in cancer metastasis-related terms. Functional studies showed that silencing of DANCR suppressed NPC cell migration and invasion, while overexpression of DANCR promoted NPC cell migration and invasion *in vitro*. Furthermore, knockdown of DANCR reduced both the inguinal lymph node metastasis and the lung metastatic colonization formation of NPC *in vivo*. Therefore, our results suggest that DANCR can function as an oncogenic lncRNA in NPC.

NF90, as a double-stranded RNA-binding protein, is transcribed from the interleukin enhancer binding factor 3 (ILF3) gene. Studies demonstrate that the NF90/NF45 complex can regulate gene expression and mRNA stability and plays an important role in RNA metabolism and viral replication [37, 38]. Here, we performed RNA pull-down assay followed by mass spectrometry analysis and found that the most enriched DANCR-binding protein was NF90 and its partner NF45. NF90, which is a specific AU-binding protein, can be recruited to the AU-rich elements (AREs) in 3'UTR of several mRNAs and then lead to mRNA degradation, stabilization or translation [26, 27, 37]. Our results showed that the deletion transcripts near the 3' region of DANCR with more AREs exhibited stronger binding potential to NF90/NF45 than those in the central and 5' regions, indicating that the AREs in the 3' region of DANCR might be more required for its interaction with

NF90/NF45. We also acknowledged that it is better to perform structure analysis or mutation assays to further confirm that NF90/NF45 actually binds to AREs in the DANCER transcript. Then, we validated the direct interaction between DANCER and NF90/NF45; they had no effect on the expression levels of each other.

To date, clinical data reveal that primary tumors arising from the nasopharynx are mostly hypoxic [39, 40], indicating that hypoxic environment may play a crucial role in NPC progression. In the present study, GSEA analysis showed that hypoxia phenotype was positively correlated with DANCER expression. Furthermore, HIF-1 $\alpha$ , a core regulator of hypoxia response [41, 42], was downregulated after DANCER depletion. Additionally, our data showed that the depletion of DANCER reduced HIF-1 $\alpha$  mRNA stability. NF90, as the most enriched DANCER-binding protein, can complex with NF45 to stabilize mRNA. Thus, we proposed a hypothesis that DANCER might increase HIF-1 $\alpha$  mRNA stability through interacting with NF90/NF45. Indeed, RIP assay confirmed the physical interaction between NF90/NF45 and HIF-1 $\alpha$  and found that DANCER could enhance this interaction. Our findings suggest that DANCER increases HIF-1 $\alpha$  mRNA stability by interacting with NF90/NF45 complex. NF90 has also been reported to cooperate with HuR and hnRNP L to increase VEGF mRNA stability [27] or compete with destabilizing proteins to regulate IL2 mRNA stability [43]. NF90 can be promoted to degrade by lncRNA-LET and then affect HIF-1 $\alpha$  expression [44]. NF90 can also form a specific complex with VEGFA mRNA to enable its mRNA translation [45]. Thus, our current study enriches our understanding of the mechanisms of NF90 involvement in regulating tumorigenesis and progression.

In conclusion, we identified DANCER as a metastasis-specific oncogenic lncRNA in NPC and further uncovered a novel pathway in which DANCER stabilized HIF-1 $\alpha$  mRNA through interacting with NF90/NF45 complex, leading to NPC metastasis. Our results also evaluated the prognostic value of DANCER and then constructed a prognostic predictive model, which would guide a more personalized therapy for NPC patients.

## Abbreviations

NPC: nasopharyngeal carcinoma; TNM: tumor-node-metastasis; lncRNA: long non-coding RNA; EBV-DNA: Epstein-Barr virus-deoxyribonucleic acid; LDH: lactate dehydrogenase; DANCER: differentiation antagonizing non-protein coding RNA; FFPE: formalin-fixed paraffin-embedded; KEGG: Kyoto Encyclopedia of Genes and

Genomes; GO: gene ontology; GSEA: gene set enrichment analysis; ARE: AU-rich element.

## Supplementary Material

Supplementary figures and tables.

<http://www.thno.org/v08p5676s1.pdf>

## Acknowledgments

This study was supported by grants from the National Natural Science Foundation of China (81773229 and 81672988), Guangdong Special Support Program (2017TQ04R754), Natural Science Foundation of Guangdong Province (2018B030306045 and 2017A030312003), Health & Medical Collaborative Innovation Project of Guangzhou City, China (201803040003), Innovation Team Development Plan of the Ministry of Education (IRT\_17R110), and Overseas Expertise Introduction Project for Discipline Innovation (111 Project, B14035). Key raw data have been uploaded to the Research Data Deposit public platform (RDD, [www.researchdata.org.cn](http://www.researchdata.org.cn)), with the approval RDD number of RDDB2018000408.

## Author Contributions

Y.L., N.L., X.W. and J.M. designed the study. X.W., X.L., Y.L., X.Y. and Q.H. conducted the experiments. X.W., X.L., Y.M., Y.W., P.Z., Y.L. and X.H. acquired and analyzed the data. N.L., J.M., Y.M., Q.H. and X.Y. provided the reagents. X.W., Y.L. and N.L. wrote the manuscript. All authors read and approve the final manuscript.

## Competing Interests

The authors have declared that no competing interest exists.

## References

1. Torre LA, Bray F, Siegel RL, et al. Global cancer statistics, 2012. *CA Cancer J Clin.* 2015; 65: 87-108.
2. Wei KR, Zheng RS, Zhang SW, et al. Nasopharyngeal carcinoma incidence and mortality in China in 2010. *Chin J Cancer.* 2014; 33: 381-387.
3. Chua M, Wee J, Hui EP, et al. Nasopharyngeal carcinoma. *Lancet.* 2016; 387: 1012-1024.
4. Zhang L, Huang Y, Hong S, et al. Gemcitabine plus cisplatin versus fluorouracil plus cisplatin in recurrent or metastatic nasopharyngeal carcinoma: a multicentre, randomised, open-label, phase 3 trial. *Lancet.* 2016; 388: 1883-1892.
5. Lee AW, Lin JC, Ng WT. Current management of nasopharyngeal cancer. *Semin Radiat Oncol.* 2012; 22: 233-244.
6. Ngeow J, Lim WT, Leong SS, et al. Docetaxel is effective in heavily pretreated patients with disseminated nasopharyngeal carcinoma. *Ann Oncol.* 2011; 22: 718-722.
7. Patel SG, Shah JP. TNM staging of cancers of the head and neck: striving for uniformity among diversity. *CA Cancer J Clin.* 2005; 55: 242-258, 261-262, 264.
8. Lee AW, Ng WT, Chan LL, et al. Evolution of treatment for nasopharyngeal cancer—success and setback in the intensity-modulated radiotherapy era. *Radiother Oncol.* 2014; 110: 377-384.
9. Chee J, Loh KS, Tham I, et al. Prognostic stratification of patients with metastatic nasopharyngeal carcinoma using a clinical and biochemical scoring system. *J Cancer Res Clin Oncol.* 2017; 143: 2563-2570.
10. Liu N, Chen NY, Cui RX, et al. Prognostic value of a microRNA signature in nasopharyngeal carcinoma: a microRNA expression analysis. *Lancet Oncol.* 2012; 13: 633-641.
11. Tang X, Li Y, Liang S, et al. Development and validation of a gene expression-based signature to predict distant metastasis in locoregionally

- advanced nasopharyngeal carcinoma: a retrospective, multicentre, cohort study. *Lancet Oncol.* 2018; 19: 382-393.
12. Ulitsky I, Bartel DP. lincRNAs: genomics, evolution, and mechanisms. *Cell.* 2013; 154: 26-46.
  13. Zhang E, Han L, Yin D, et al. H3K27 acetylation activated-long non-coding RNA CCAT1 affects cell proliferation and migration by regulating SPRY4 and HOXB13 expression in esophageal squamous cell carcinoma. *Nucleic Acids Res.* 2017; 45: 3086-3101.
  14. DeOcesano-Pereira C, Amaral MS, Parreira KS, et al. Long non-coding RNA INXS is a critical mediator of BCL-XS induced apoptosis. *Nucleic Acids Res.* 2014; 42: 8343-8355.
  15. Rodriguez-Mateo C, Torres B, Gutierrez G, et al. Downregulation of Lnc-Spry1 mediates TGF-beta-induced epithelial-mesenchymal transition by transcriptional and posttranscriptional regulatory mechanisms. *Cell Death Differ.* 2017; 24: 785-797.
  16. Wang X, Sun W, Shen W, et al. Long non-coding RNA DILC regulates liver cancer stem cells via IL-6/STAT3 axis. *J Hepatol.* 2016; 64: 1283-1294.
  17. Prensner JR, Zhao S, Erho N, et al. RNA biomarkers associated with metastatic progression in prostate cancer: a multi-institutional high-throughput analysis of SChLAPI. *Lancet Oncol.* 2014; 15: 1469-1480.
  18. Liu B, Sun L, Liu Q, et al. A cytoplasmic NF-kappaB interacting long noncoding RNA blocks IkappaB phosphorylation and suppresses breast cancer metastasis. *Cancer Cell.* 2015; 27: 370-381.
  19. Wen X, Tang X, Li Y, et al. Microarray Expression Profiling of Long Non-Coding RNAs Involved in Nasopharyngeal Carcinoma Metastasis. *Int J Mol Sci.* 2016; 17:1956.
  20. Kretz M, Webster DE, Flockhart RJ, et al. Suppression of progenitor differentiation requires the long noncoding RNA ANCR. *Genes Dev.* 2012; 26: 338-343.
  21. Yuan SX, Wang J, Yang F, et al. Long noncoding RNA DANCR increases stemness features of hepatocellular carcinoma by derepression of CTNBN1. *Hepatology.* 2016; 63: 499-511.
  22. Mao Z, Li H, Du B, et al. LncRNA DANCR promotes migration and invasion through suppression of lncRNA-LET in gastric cancer cells. *Biosci Rep.* 2017; 37: BSR20171070.
  23. Livak KJ, Schmittgen TD. Analysis of relative gene expression data using real-time quantitative PCR and the 2(-Delta Delta C(T)) Method. *Methods.* 2001; 25: 402-408.
  24. Zheng J, Huang X, Tan W, et al. Pancreatic cancer risk variant in LINC00673 creates a miR-1231 binding site and interferes with PTPN11 degradation. *Nature Genetics.* 2016; 48: 747-757.
  25. Sun TT, He J, Liang Q, et al. LncRNA GClnc1 promotes gastric carcinogenesis and may act as a modular scaffold of WDR5 and KAT2A complexes to specify the histone modification pattern. *Cancer Discovery.* 2016; 6: 784-801.
  26. Kuwano Y, Pullmann R, Marasa BS, et al. NF90 selectively represses the translation of target mRNAs bearing an AU-rich signature motif. *Nucleic Acids Research.* 2010; 38: 225-238.
  27. Vumbaca F, Phoenix KN, Rodriguez-Pinto D, et al. Double-stranded RNA-binding protein regulates vascular endothelial growth factor mRNA stability, translation, and breast cancer angiogenesis. *Mol Cell Biol.* 2008; 28: 772-783.
  28. Ye J, Jin H, Pankov A, et al. NF45 and NF90/NF110 coordinately regulate ESC pluripotency and differentiation. *RNA.* 2017; 23: 1270-1284.
  29. Zhang K, Shi H, Xi H, et al. Genome-wide lncRNA microarray profiling identifies novel circulating lncRNAs for detection of gastric cancer. *Theranostics.* 2017; 7: 213-227.
  30. Liu YR, Jiang YZ, Xu XE, et al. Comprehensive transcriptome profiling reveals multigene signatures in triple-negative breast cancer. *Clin Cancer Res.* 2016; 22: 1653-1662.
  31. Antonov J, Goldstein DR, Oberli A, et al. Reliable gene expression measurements from degraded RNA by quantitative real-time PCR depend on short amplicons and a proper normalization. *Lab Invest.* 2005; 85: 1040-1050.
  32. Kong H, Zhu M, Cui F, et al. Quantitative assessment of short amplicons in FFPE-derived long-chain RNA. *Sci Rep.* 2014; 4: 7246.
  33. Kobayashi R, Miyagawa R, Yamashita H, et al. Increased expression of long non-coding RNA XIST predicts favorable prognosis of cervical squamous cell carcinoma subsequent to definitive chemoradiation therapy. *Oncol Lett.* 2016; 12: 3066-3074.
  34. Nie Y, Liu X, Qu S, et al. Long non-coding RNA HOTAIR is an independent prognostic marker for nasopharyngeal carcinoma progression and survival. *Cancer Sci.* 2013; 104: 458-464.
  35. Fu WM, Lu YF, Hu BG, et al. Long noncoding RNA Hotair mediated angiogenesis in nasopharyngeal carcinoma by direct and indirect signaling pathways. *Oncotarget.* 2016; 7: 4712-4723.
  36. He Y, Jing Y, Wei F, et al. Long non-coding RNA PVT1 predicts poor prognosis and induces radioresistance by regulating DNA repair and cell apoptosis in nasopharyngeal carcinoma. *Cell Death Dis.* 2018; 9: 235.
  37. Castella S, Bernard R, Corno M, et al. IIf3 and NF90 functions in RNA biology. *Wiley Interdiscip Rev RNA.* 2015; 6: 243-256.
  38. Schmidt T, Friedrich S, Golbik RP, et al. NF90-NF45 is a selective RNA chaperone that rearranges viral and cellular riboswitches: biochemical analysis of a virus host factor activity. *Nucleic Acids Res.* 2017; 45: 12441-12454.
  39. Yeh SH, Liu RS, Wu LC, et al. Fluorine-18 fluoromisonidazole tumour to muscle retention ratio for the detection of hypoxia in nasopharyngeal carcinoma. *Eur J Nucl Med.* 1996; 23: 1378-1383.
  40. Hong B, Lui VW, Hashiguchi M, et al. Targeting tumor hypoxia in nasopharyngeal carcinoma. *Head Neck.* 2013; 35: 133-145.
  41. Rankin EB, Giaccia AJ. Hypoxic control of metastasis. *Science.* 2016; 352: 175-180.
  42. Higgins DF, Kimura K, Bernhardt WM, et al. Hypoxia promotes fibrogenesis *in vivo* via HIF-1 stimulation of epithelial-to-mesenchymal transition. *J Clin Invest.* 2007; 117: 3810-3820.
  43. Shim J, Lim H, R YJ, et al. Nuclear export of NF90 is required for interleukin-2 mRNA stabilization. *Mol Cell.* 2002; 10: 1331-1344.
  44. Yang F, Huo XS, Yuan SX, et al. Repression of the long noncoding RNA-LET by histone deacetylase 3 contributes to hypoxia-mediated metastasis. *Mol Cell.* 2013; 49: 1083-1096.
  45. Yao P, Potdar AA, Ray PS, et al. The HILDA complex coordinates a conditional switch in the 3'-untranslated region of the VEGFA mRNA. *PLoS Biol.* 2013; 11: e1001635.2.